Nanoscale Patterning of Organic Monolayers by Catalytic Stamp Lithography: Scope and Limitations

Hidenori Mizuno and Jillian M. Buriak*

Department of Chemistry, University of Alberta, and the National Institute for Nanotechnology, National Research Council, Edmonton, Alberta, T6G 2G2, Canada

ABSTRACT Developing a method to pattern organic molecules, particularly on the sub-100-nm scale, is of wide interest in current nanoscience for a broad range of technological applications. Because of the efficiency and simplicity of soft lithography, here we describe in detail the process for synthesizing and applying catalytic stamp lithography, a process that can easily produce sub-100-nm patterns on surfaces; in this work, the approach is demonstrated on silicon. Catalytic stamps were fabricated through a two-step procedure in which the nanoscale pattern of catalysts is produced via a self-assembled block-copolymer-templated synthesis of metallic nanostructures on SiO_x/Si supports, followed by the production of the poly(dimethylsiloxane) (PDMS) stamp on top of the as-patterned metals. Simply peeling off the as-formed PDMS stamp removes the metallic nanostructures, leading to the functional stamp. Two different patterns, pseudohexagonal and linear Pt nanoarrays, were produced from a single block copolymer, PS_{125000}-*b*-$P2VP_{58500}$, by controlling the morphology of thin-film templates through tetrahydrofuran vapor annealing. When terminal alkenes, alkynes, or aldehydes with different functionalities were used as molecular inks, these Pt nanopatterns on catalytic stamps were translated into corresponding molecular arrays on Si(111)-H and Si(100)-H_x surfaces because catalytic hydrosilylation took place exclusively underneath patterned Pt nanostructures. With this straightforward approach, the resolution limit of conventional microcontact printing (~100 nm) could be downsized to a sub-20-nm scale, while maintaining the advantages of stamp-based patterning (i.e., large-area, high-throughput capabilities and low cost).

KEYWORDS: nanoscale patterning • organic monolayer • soft lithography • PDMS stamp • hydrosilylation • silicon surface • block copolymer

INTRODUCTION

The ability to control the formation of organic nanostructures in terms of size, shape, composition, and location on the sub-100-nm scale is of growing importance in the field of nanoscience because of its promise in developing molecular-scale engineering, including electronics (1), optics (2), fluidics (3), mechanics (4), and bioanalysis (5). Interfacing a wide variety of organic and biological molecules with a range of technologically important substrates would open new designs of architectures with improved and/or new functionalities. While a number of fabrication techniques are currently available (6), the construction of hybrid nanostructures remains a challenge both technically and practically. The longstanding top-down fabrication by photolithography is, for example, viable for producing inorganic-based nanostructures (6, 7) but is less ideal for handling delicate organic and biological materials because of the relatively severe conditions required (8). Scanning probe-mediated bottom-up approaches, including scanning tunneling microscopy (STM)-based atomic/molecular manipulation (9) and dip-pen nanolithography (10), can routinely produce sub-100-nm features with various materials, but expansion to parallel operations for mass production is still in its infancy (10c, 10d). More critically, these methods will continue to require significant investments to develop the technologies, instruments, and infrastructure, leading to a consideration of alternative strategies from an economical perspective (11).

In a separate vein from these technologically sophisticated methodologies, some of the classic types of "low-tech" routes, such as molding (embossing) and stamping (printing), also have the potential to create nanoscale features in a high-throughput, large-area, and cost-effective manner (8a, 8b). Soft lithography (12) refers to a series of such techniques that utilize elastomeric polymers, typically poly(dimethylsiloxane) (PDMS), as molds, masks, or stamps; the development of applications of soft lithography to nanofabrication has been actively pursued worldwide (8b). Microcontact printing (μCP) is a stamp-based soft-lithographic technique that is widely used to produce organic and biological patterns on various solid supports, including nonflat surfaces (8c, 13). Accurate pattern transfer is routinely applied on the microscale, and while much smaller features have been demonstrated, it is technically challenging to achieve sub-100-nm features via μCP (8c, 13d, 13e). Conventional μCP usually relies on either spontaneous chemisorption or simple physisorption to deposit molecular "inks" onto target surfaces; both processes can be significantly influenced by ink diffusion (14). In addition, the capabilities of stamps to replicate the topographic features from photo-

* E-mail: jburiak@ualberta.ca.
Received for review September 4, 2009 and accepted November 16, 2009
DOI: 10.1021/am900602m

litographically created masters and to maintain them without deformation during the stamping procedure also play significant roles with regard to the final sizes of the transferred features (15). In order to facilitate nanoscale patterning by μCP, these ink- and stamp-based challenges need to be overcome. For instance, to achieve a diffusion-free process, the use of high molecular weight materials such as inks has been explored (14a, 16), and less-deformable composite structures have been developed to improve the stamp stability (17). Huck and co-workers have successfully carried out "nanocontact" printing by combining these two approaches, where sub-50-nm features were obtained (18). Alternatively, topographically flat (but chemically patterned) stamps (19) have also been adopted in nanoscale patterning (19d, 19f).

A possible route to achieve nanoscale resolution, via μCP, would be the utilization of more nanoscale site-specific reactions, directed by catalysts in the stamp itself, to formulate chemical patterns. This approach has been inspired from work in which catalytic transformations of surface species have been performed using catalytic scanning probes to produce sub-100-nm-scale patterns, and previous examples include Pt- (20) or Pd-catalyzed hydrogenation (21), Pd-catalyzed hydrosilylation (21), acid-catalyzed hydrolysis (22), and Pd-catalyzed C−C bond-forming reactions (the Suzuki coupling and the Heck reaction) (23). The integration of catalysis and μCP has been proposed recently. For example, Li et al. used oxygen plasma-treated PDMS stamps to pattern a silyl ether terminated self-assembled monolayer on Au via acid-catalyzed hydrolysis (24). Snyder and co-workers incorporated enzymes on a patterned poly(acrylamide)-based stamp and demonstrated site-selective hydrolytic cleavage of a fluorescent dye attached to a DNA monolayer (25). Spruell et al. performed Cu-catalyzed azide−alkyne cyclization on azide-terminated surfaces with Cu-coated PDMS stamps (26). In these papers, the minimum feature sizes accessible are within the micrometer range. In order to integrate patterned nanoscale metallic catalysts with PDMS, we utilized block-copolymer-based self-assembly to produce the desired patterns and then incorporated them into a PDMS stamp. Via our approach, first the metallic catalyst pattern is produced on a rigid support and then the flexible PDMS is mixed and cured over top, yielding a stamp that can be applied for catalytic stamp lithography (27).

In this present report, we describe the comprehensive study on catalytic stamp lithography, including detailed procedures regarding the fabrication of catalytic stamps. Surfaces of PDMS substrates were decorated with catalytically active Pt nanostructures in spatially defined fashions via the use of the commercially available family of block copolymers, polystyrene-*block*-poly(2-vinylpyridine). This family of block copolymers has been shown to form a broad range of morphologies (spheres, vertical/horizontal cylinders, lamellae, and so on) (28) with different size ranges (typically 10−100 nm) (28), although any self-assembly system that could result in metallic nanopatterns could be used. In this work, both hexagonally close-packed and linearly nanopatterned Pt PDMS catalytic stamps were created and employed to demonstrate site-specific hydrosilylation on H-terminated Si(111) and Si(100) substrates, and nanopatterns of hydrosilylated alkene, alkyne, or aldehyde molecules were produced. Characterization of the as-obtained molecular arrays was obtained via tapping-mode atomic force microscopy (AFM) imaging, X-ray photoelectron spectroscopy (XPS) analysis, and stability tests under organic and aqueous solutions. Pattern creation was also attempted on alkene-terminated Si substrates using silanes as molecular inks to determine the scope and limitations of hydrosilylation-based catalytic stamp lithography.

EXPERIMENTAL SECTION

Generalities. Unless otherwise noted, all of the experiments were performed under ambient conditions. Teflon beakers and tweezers were used exclusively during cleaning and etching of the Si wafers. Si(111) (p-type, B-doped, $\rho = 1-10\ \Omega$ cm, and thickness = 600−650 μm) and Si(100) (p-type, B-doped, $\rho = 0.01-0.02\ \Omega$ cm, and thickness = 600−650 μm) wafers were purchased from MEMC Electronic Materials, Inc. Water was obtained from a Millipore system (resistivity = 18.2 MΩ). Aqueous HCl (36.5−38%, Baker-analyzed ACS reagent), NH_4OH (29%, Finyte), H_2O_2 (30%, CMOS), HF (49%, CMOS), and NH_4F (40%, CMOS) were purchased from J. T. Baker. The block copolymers used in this study were of the composition polystyrene-*block*-poly(2-vinylpyridine) with the following molecular weights: polystyrene = 125 000 g/mol and poly(2-vinylpyridine) = 58 500 g/mol (PS_{125000}-*b*-$P2VP_{58500}$; PDI = 1.05), obtained from Polymer Source, Inc. Two kinds of PDMSs, termed h- and 184-PDMS, were used, and the prepolymers of h-PDMS (VDT-731, HMS-301, and SIP6831.1) were obtained from Gelest Corp., while those of 184-PDMS (Sylgard 184) were obtained from Dow Corning. Trichloro(1*H*,1*H*,2*H*,2*H*-perfluorooctyl)silane (98%), 2,4,6,8-tetramethyl-2,4,6,8-tetravinylcyclotetrasiloxane, 1*H*,1*H*,2*H*-perfluoro-1-decene (99%), 10-undecynoic acid (95%), undecanal (97%), benzaldehyde (>98.0%, purum), phenylsilane (97%), dimethylphenylsilane (>98%), dimethyloctadecylsilane (97%), CH_2Cl_2 (>99.9%, Chromasolv, for HPLC), and toluene (>99.9%, Chromasolv, for HPLC) were purchased from Sigma-Aldrich. $Na_2PtCl_4 \cdot xH_2O$ was obtained from Strem Chemicals. Optima-grade tetrahydrofuran (THF), methanol, and 2-propanol were purchased from Fisher. All of the reagents listed above were used as-received. 1,4-Dioxane (99%, Caledon Laboratories Ltd.), 1-dodecene (95%, Sigma-Aldrich), octenyltrichlorosilane (96%, mixture of isomers, Sigma-Aldrich), phenylacetylene (96%, Sigma-Aldrich), 4-vinylpyridine (95%, Sigma-Aldrich), and 1-octadecanethiol (98%, Sigma-Aldrich) were purified according to the standard methods (29) before use.

Silicon Cleaning Procedures. Pieces of Si(111) or Si(100) (~1 cm^2) were degreased in methanol using an ultrasonic bath for 15 min. The wafers were then cleaned via standard RCA cleaning procedures (30): the wafers were first immersed in a solution of $H_2O/NH_4OH/H_2O_2$ (5/1/1) and heated (80 °C) for 15 min. After the wafers were rinsed with excess water, they were immersed in another solution of $H_2O/HCl/H_2O_2$ (6/1/1) and reheated (80 °C) for 15 min. The wafers were again rinsed with an excess amount of water and dried with a stream of nitrogen.

Preparation of Block Copolymer Solutions. A block copolymer, PS_{125000}-*b*-P2 VP_{58500}, was dissolved in toluene and stirred for 1 h at room temperature to make 1.0 wt % solutions. The solutions were allowed to sit for 24 h prior to use to complete the micelle formation.

Preparation of Block-Copolymer Thin-Film Templates on SiO_x/Si Substrates. An RCA-cleaned Si sample was spin-coated (model WS-400B-6NPP-Lite, Laurell Technologies) with

10 μL of a block-copolymer solution at 6000 rpm for 40 s. Subsequently, solvent annealing was carried out for ~20 h in a chamber, an inverted 500 mL crystallization dish, and 5 mL of THF in a small beaker placed on top of aluminum-foil-covered papers (Supporting Information, Figure S1). By controlling the degree of sealing of the annealing system, either a pseudohexagonal or a linear template was produced. To obtain the pseudohexagonal pattern, the polymer-coated sample was placed in the chamber, and a 500 g mass was placed on top of the inverted dish to loosely seal the chamber. Alternatively, a 2 kg mass was used to prepare the linearly patterned template by sealing the chamber tightly.

Preparation of Pt Nanostructures on SiO_x/Si Substrates. A block-copolymer-templated sample was immersed in 10 mM Na_2PtCl_4(aq) containing 0.9% HCl and 3 h, rinsed thoroughly with a copious amount of water, and dried with a stream of nitrogen. The Pt^{2+}-loaded sample was then treated with Ar/H_2 plasma (Harrick PDC 32G, 18W) at 1.5 Torr for 30 min to reduce Pt^{2+} to Pt^0 and to remove block-copolymer templates.

Preparation of Catalytic Stamps. A Pt-patterned SiO_x/Si substrate was immediately transferred into a desiccator containing an open vial of trichloro(1*H*,1*H*,2*H*,2*H*-perfluorooctyl)-silane (15 μL) after the plasma treatment. The desiccator was closed and pumped to ~1 Torr to carry out vapor-phase deposition of the corresponding siloxane monolayer on SiO_x. After 1 h with static vacuum, the sample was exposed to an ambient atmosphere and washed with ethanol and water to remove polymerized siloxane residues. This sample was next spin-coated with h-PDMS (17c, 17d), a mixture of 0.38 g of a vinylsilane prepolymer (VDT-731), 2 μL of a Pt catalyst (platinum divinyltetramethyldisiloxane, SIP6831.1), 12 μL of a modulator (2,4,6,8-tetramethyltetravinylcyclotetrasiloxane), and 0.12 mL of a hydrosilane prepolymer (HMS-301), at 1000 rpm for 40 s, and then cured at 65 °C for 30 min. After the first curing, degassed 184-PDMS, a 10/1 mixture of Sylgard 184 prepolymer and curing agent, was poured onto the h-PDMS-covered sample, degassed, and cured again at 65 °C at least for 3 h. After the second curing, the whole sample was allowed to cool to room temperature, and then the composite PDMS was carefully peeled off from the SiO_x/Si substrate. In order to remove low-molecular-weight PDMS, the catalytic stamps were extracted overnight with hexane, dried under vacuum, and sonicated three times in a freshly prepared ethanol/water = 2/1 solution for 5 min (31). This washing process was repeated three times, and the washed catalytic stamps were kept under vacuum until use.

Preparation of H-Terminated Si(111)/Si(100). RCA-cleaned Si(111) or Si(100) samples were immersed in degassed 40% NH_4F(aq) for Si(111) (32) or 1% HF(aq) for Si(100) for 5 min. The hydride-terminated surfaces were immediately dipped into water for 10 s and dried with a stream of nitrogen.

Patterning of H-Terminated Si Surfaces via Hydrosilylation. Several droplets of a 5 mM solution of alkene/alkyne/aldehyde in 1,4-dioxane was placed on a Pt catalytic stamp for 1 min, and then solution was gently blown off with a nitrogen stream. The inked stamp was applied to a freshly prepared H-terminated Si(111) or Si(100) sample and pressed lightly for 20 min using a homemade stamping apparatus. After stamping, PDMS was released from the Si sample, and the resulting Si sample was rinsed with dichloromethane and immediately submitted to further experiments/analyses.

Deactivation of Pt Catalytic Stamps. A Pt catalytic stamp was immersed in a 1 mM ethanolic solution of 1-octadecanethiol for 24 h to form a self-assembled monolayer on the Pt nanostructures. The resulting stamp was then rinsed thoroughly with ethanol, and the washed stamp was immediately used for the lithographic experiment described above.

Preparation of an Alkene-Terminated Siloxane Monolayer on SiO_x/Si(100). An RCA-cleaned Si(100) sample was immersed in a 0.5% (v/v) toluene solution of octenyltrichlorosilane for 24 h. The surface of an octenyltrichlorosilane-treated sample was gently swabbed with a toluene-soaked cotton swab to eliminate polymerized siloxane residues, then washed in toluene using an ultasonication bath for 10 min, and rinsed with ethanol and water prior to use.

Attempted Patterning on Alkene-Terminated Surfaces. The procedure was similar to the patterning on H-terminated Si surfaces: silane and alkene-terminated surfaces were used in place of alkene/alkyne/aldehyde and H-terminated surfaces, respectively. For stamping at elevated temperature (65 °C), the inked Pt catalytic stamp was applied on an alkene-terminated surface at room temperature, and the whole system was immediately placed in the preheated oven for 20 min.

Surface Characterization. The samples obtained in this study were characterized by AFM, scanning electron microscopy (SEM), and XPS. AFM images were taken with a Digital Instruments/Vecco Nanoscope IV (tapping mode) using commercially available Si cantilevers under ambient conditions. SEM was performed with Hitachi S-4800 field emission scanning electron microscopy using an electron energy of 10 keV under high-vacuum conditions ($<10^{-8}$ Torr). XPS was taken on a Kratos Axis 165 X-ray photoelectron spectrometer using a monochromatic Al Kα with a photon energy of 1486.6 eV under high-vacuum conditions ($<10^{-8}$ Torr), and ejected X-rays were measured at 0° from the surface normal. To avoid surface charging for PDMS samples, the charge neutralizer was used. The XPS signals were calibrated on the basis of Si $2p_{3/2}$ (99.3 eV) or O 1s (532.0 eV).

RESULTS AND DISCUSSION

Fabrication of Catalytic Stamps. The stamps used in this study, termed catalytic stamps, consist of flexible PDMS supports whose surfaces were patterned with metallic nanostructures produced via a self-assembly-based approach. This design allows localized catalysis by nanostructured metals (33) upon stamping on an appropriate surface, where intimate contact is ensured by the elastomeric nature of PDMS (12). As illustrated in Scheme 1, the general procedure to fabricate catalytic stamps is divided into two steps: (1) the synthesis of metallic nanopatterns on native oxide-capped Si (SiO_x/Si) via the use of self-assembled block-copolymer templates (28a, 34, 35) and (2) the transfer of as-synthesized metallic nanopatterns onto PDMS surfaces through a simple peel-off step (27). A similar block-copolymer-templated strategy has been described by Spatz et al. to pattern Au nanoparticles on flexible hydrogel supports for cell adhesion studies (36). Because photolithography and other clean-room-based fabrication techniques are not required to develop the parent master, the entire process can be carried out with a standard laboratory apparatus (laboratory ambient, benchtop).

In the first step (Scheme 1, top row), a thin monolayer of self-assembled block copolymer, PS_{125000}-*b*-$P2VP_{58500}$, was prepared on a SiO_x/Si substrate. Spin coating of micellized PS_{125000}-*b*-$P2VP_{58500}$ in toluene (1.0 wt %) resulted in pseudohexagonally organized P2VP cores surrounded by a PS matrix (Supporting Information, Figure S2). The order of the hexagonal pattern was enhanced by solvent (THF) annealing for ~20 h (34d) (Supporting Information). This organized block-copolymer micelle monolayer then acts as the template to produce the metallic nanoarrray via immersion in a 10 mM aqueous solution of the desired metallic salt; in the example here, the salt is Na_2PtCl_4 in a solution

Scheme 1. General Procedure for the Fabrication of Catalytic Stamps[a]

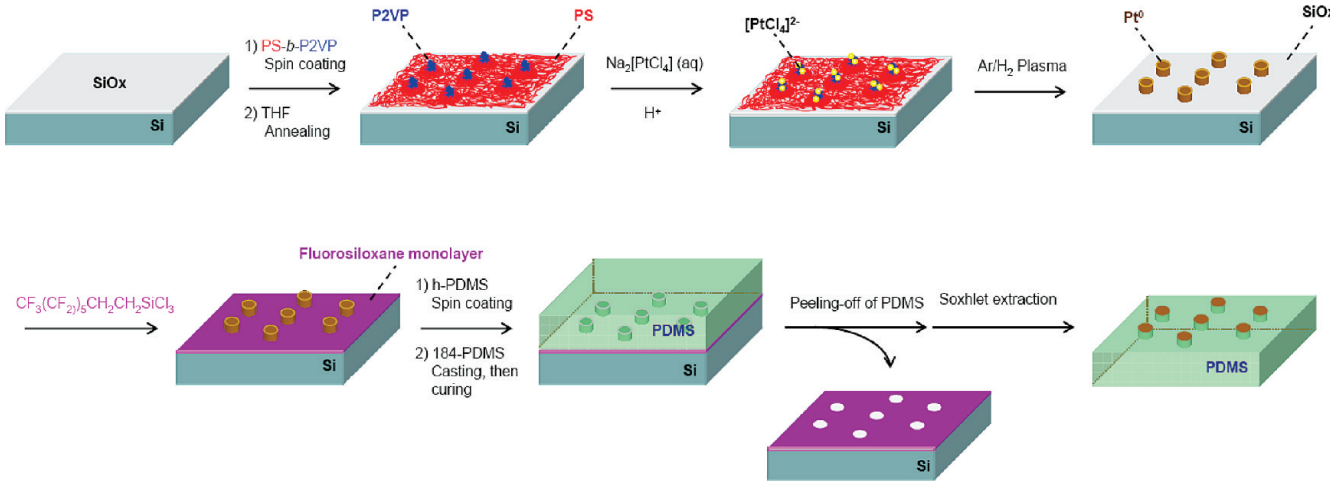

[a] (Top row) Block-copolymer (PS-*b*-P2VP)-templated synthesis of a Pt nanopattern on oxide-capped Si. (Bottom row) Transfer of a Pt nanopattern onto the PDMS surface through a peel-off approach.

containing 0.9 % HCl. The length of time for immersion was 3 h, conditions under which the precursor anionic Pt^{2+} salt is selectively loaded within the P2VP domains. Under the acidic conditions employed (pH = 0.9), the pyridyl groups in the P2VP domains would be fully protonated (pK_a of P2VP in an aqueous solution is 4−4.5) (37); therefore, the negatively charged Pt complex, $[PtCl_4]^{2-}$, coordinates to positively charged pyridinium groups through electrostatic interactions (34). Afterward, an Ar/H_2 plasma treatment was performed to remove the PS_{125000}-*b*-$P2VP_{58500}$ template, and the Pt^{2+} ions were simultaneously reduced to Pt^0 without introducing disorder to the original geometry of the PS-*b*-P2VP pattern (28a, 34, 35).

In the second step (Scheme 1, bottom row), the Pt-patterned sample was exposed to vapor of trichloro(1*H*,1*H*,2*H*,2*H*-perfluorooctyl)silane under reduced pressure to prepare a fluorinated alkylsiloxane monolayer on the exposed SiO_x regions (38). Subsequently, two kinds of PDMS, termed h- and 184-PDMS, were mounted on the sample first by spin coating a thin layer of h-PDMS, followed by coating with 184-PDMS, to form double-layered PDMS (17d). After thermal curing at 65 °C for 3 h, the composite PDMS was carefully peeled off from the SiO_x/Si surface to afford the catalytic stamp. Because of the highly fluorinated phase formed on SiO_x on the SiO_x/Si substrate, the master could be smoothly separated from the PDMS stamp (38), while the Pt nanostructure was physically captured by h-PDMS and dislocated from the original SiO_x interface. It was found that the use of h-PDMS was essential to facilitate the complete transfer of the Pt nanostructure; partial transfer of Pt occurred when only 184-PDMS was used. The higher Young's modulus of h-PDMS (~9 MPa) (17c), compared to 184-PDMS (~3 MPa) (17c), assisted in firmly taking hold of the Pt nanostructures produced on SiO_x/Si. Finally, the catalytic stamp prepared through this approach was submitted to a Soxhlet extraction process using hexane to remove low-molecular-weight PDMS (31) (see the Experimental Section). It should be emphasized that no disappearance of the Pt nanostructure from PDMS was observed by AFM even after this harsh cleaning process.

Figure 1 shows AFM images of the original hexagonal polymer templates, the SEM images of Pt patterns on SiO_x/Si produced via the metallization approach, and AFM images of the resulting Pt catalytic stamps. The hexagonal geometry of the P2VP domains in the parent PS_{125000}-*b*-$P2VP_{58500}$ template was clearly translated into metallic Pt on SiO_x/Si and then finally into metallic Pt on PDMS. The final domain size (18 nm) and the center-to-center spacing (64 nm) of the Pt pattern in the catalytic stamp were almost identical with those of the P2VP pattern in the template. The efficiency of transferring the Pt nanostructure from SiO_x/Si to PDMS was usually very good, but occasionally untransferred Pt was observed on the original SiO_x/Si by AFM (Supporting Information, Figure S3). Because good and consistent contact between the Pt nanopattern, on the PDMS stamp, and the surface during stamping is a necessity, the morphology of the Pt nanostructures is particularly important. Cross-sectional SEM images of the bare Pt nanostructures on the SiO_x/Si interface reveal the truncated cone shape of the nanoparticles, with a flat Pt face that forms on the smooth single-crystal silicon surface. AFM imaging of the PDMS/Pt nanostructure stamp (Figure 1c) reveals the expected pattern produced from the block-copolymer template; the flat nature of Pt nanoparticles cannot be verified, however, by AFM because of tip convolution effects (Supporting Information, Figure S4).

In addition to a pseudohexagonal metallic pattern, a linear Pt nanostructure (34b, 34c) was also created on PDMS (Supporting Information). AFM images of the linear template, SEM images of Pt patterns on SiO_x/Si, and AFM images of the resulting Pt catalytic stamp are shown in Figure 2. As before with the pseudohexagonally close-packed array, conversion of the P2VP pattern into the Pt pattern was confirmed on both SiO_x/Si and PDMS. The width of the Pt lines and their center-to-center spacing on the PDMS catalytic stamp were 15 and 59 nm, respectively, consistent with the width and interdomain distance of cylindrical P2VP domains in the parent polymer template.

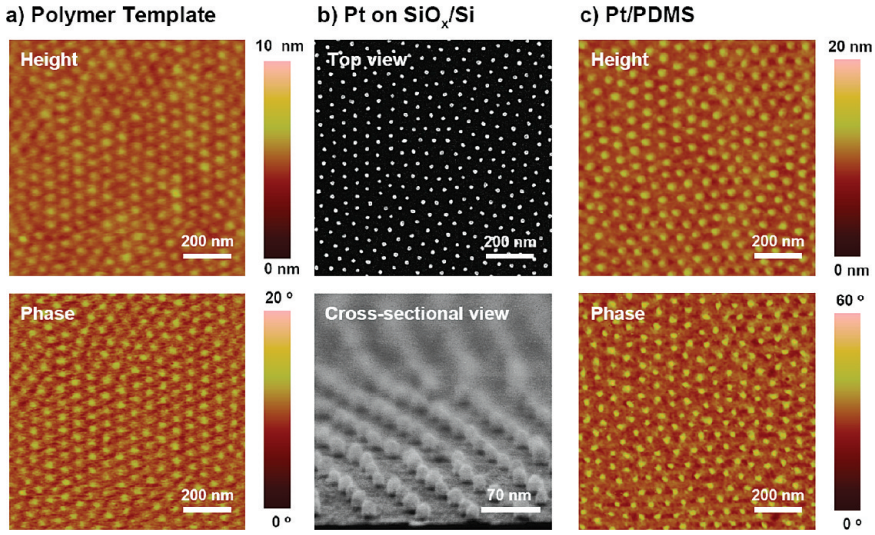

FIGURE 1. (a) AFM height and phase images of a pseudohexagonally patterned PS_{125000}-*b*-$P2VP_{58500}$ template produced on SiO_x/Si(111). (b) SEM top and cross-sectional view images of hexagonally patterned Pt nanostructures obtained from part a. (c) AFM height and phase images of the Pt catalytic stamp, obtained by transferring the Pt nanostructures of part b onto PDMS by a peel-off approach.

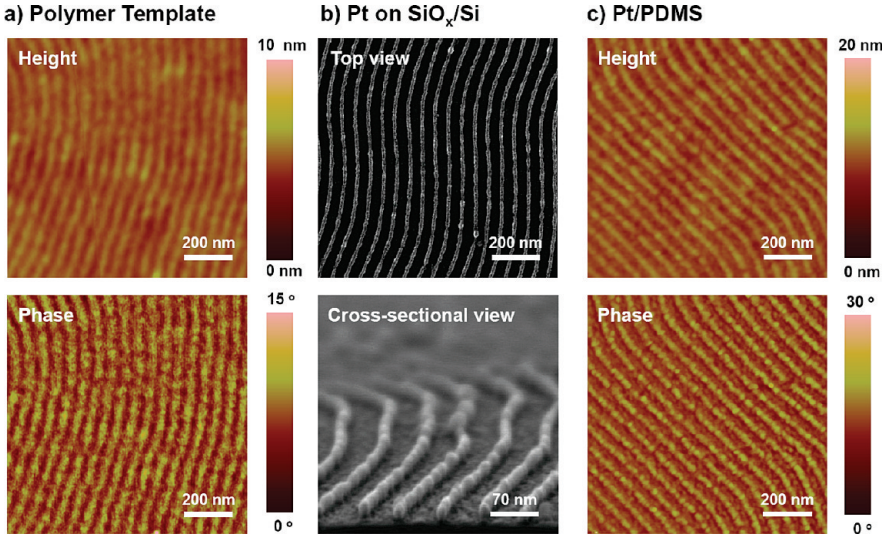

FIGURE 2. (a) AFM height and phase images of a linearly patterned PS_{125000}-*b*-$P2VP_{58500}$ template produced on SiO_x/Si(111). (b) SEM top and cross-sectional view images of linearly patterned Pt nanostructures obtained from part a. (c) AFM height and phase images of the Pt catalytic stamp, obtained by transferring the Pt nanostructures of part b onto PDMS by a peel-off approach.

XPS measurements were carried out on a Pt catalytic stamp to investigate the status of Pt metallic nanostructures embedded on a PDMS support. The main peaks found in the survey scan (Figure 3a) were Si 2p (102 eV), C 1s (284 eV), and O 1s (532 eV), all of which correspond to bulk PDMS (39). Although the signal from Pt was small in the survey scan because of the low surface coverage on the sample, the high-resolution XPS spectrum of the Pt 4f region (Figure 3b) revealed the existence of Pt with a binding energy of Pt $4f_{7/2}$ = 71.4 eV, which is in good agreement with the expected value for Pt^0 (40). The formation of platinum oxides (PtO_2 and/or PtO) was not detected despite the handling of catalytic stamps under an ambient atmosphere, although the formation of a thin-layer oxide cannot be ruled out. This may, however, not be a problem for use in catalytic stamp lithography, as discussed in the next section, because platinum oxide catalyzed hydrosilyation has been reported previously (41).

Catalytic Stamp Lithography. The catalytic stamps fabricated as described above were employed to perform nanoscale patterning of organic monolayers on silicon surfaces. In a preliminary communication, we demonstrated hydrosilylation-based catalytic stamp lithography of alkene and alkyne molecules on H_x-terminated Si(111) and Si(100) surfaces using Pd catalytic stamps (27). Some of the highlights in that work were as follows: (1) pseudohexagonal nanopatterns of organic monolayers could be produced with features as small as 20 nm over a large area (~1 cm^2) in a relatively short time (<30 min); (2) patterns could be tuned with respect to spot sizes, center-to-center spacings, and chemical properties (hydrophobicity/hydrophilicity); (3) patterned surfaces could be utilized as platforms for more complicated nanoarchitectures (i.e., selective capture of Au nanoparticules on a thiol-patterned surface); (4) Pd catalytic stamps could be reused multiple times.

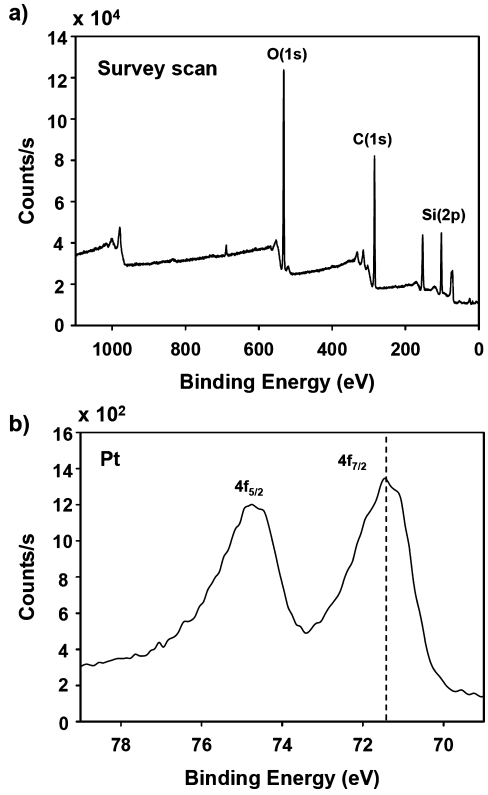

FIGURE 3. XPS spectra of a Pt catalytic stamp: (a) survey scan; (b) high-resolution XPS spectrum of the Pt 4f region. The dashed line corresponds to the known value for metallic Pt.

In order to expand the scope of catalytic stamp lithography with respect to hydrosilylation, we utilized Pt catalytic stamps in the present report because Pt is historically the most actively investigated metal for hydrosilylation catalysis (42). In addition, an aldehyde functionality (43) was also included in the list of molecular inks, in addition to alkenes and alkynes. Scheme 2 outlines the general procedure for catalytic stamp lithography: A Pt catalytic stamp was coated with a dilute (typically 5 mM) solution of alkene, alkyne, or aldehyde in 1,4-dioxane for 1 min, and then the remaining ink was gently blown off with a stream of nitrogen (inking). This inked stamp was then applied to a freshly prepared H-terminated Si(111) or Si(100) surface under ambient laboratory conditions (stamping). The stamp was typically held stationary on the surface for 20 min under continuous pressure, and finally the catalytic stamp was released from the silicon surface, yielding the patterned organic monolayer produced via hydrosilylation (pattern formation via localized catalysis).

Figure 3 shows the tapping-mode AFM height and phase images of stamped H-terminated Si(111) [Si(111)-H] or Si(100) [Si(100)-H_x] surfaces using hexagonally or linearly patterned Pt catalytic stamps (see Figure 1c or 2c, respectively). Eight varieties of molecular inks were tested under the conditions described above, containing terminal C═C, C≡C, or C═O groups, to produce the corresponding hydrosilylated alkyl, alkenyl, or alkoxy groups; all of the resulting patterns appeared as positive features in the height mode in the AFM images. As mentioned earlier, the surfaces of Pt nanostructures are believed to be flat and are therefore able to make good contact with the precursor H-terminated Si surfaces. Because highly localized catalysis took place exclusively underneath the nanopatterned Pt during stamping, the size (∼18 nm) and center-to-center spacing (∼64 nm) for the hexagonal pattern or the width (∼15 nm) and interline distance (∼59 nm) for linear patterns were nearly identical with the original Pt patterns of the catalytic stamp (vide supra) and thus were not apparently affected by ink diffusion or stamp deformation. Depending on the chemical nature of terminal functional groups in the stamped molecules relative to the surrounding H-terminated Si, negative (more hydrophobic) patterns (27) were obtained in the case of 1-dodecene (a), 1*H*,1*H*,2*H*-perfluoro-1-dodecene (c), phenylacetylene (d), undecanal (f), and benzaldehyde (g) in the phase images, while positive (more hydrophilic) patterns (27) were obtained in the case of 4-vinylpyridine (b) and 10-undecynoic acid (e).

In contrast, when dodecane was used as an ink, pattern transfer did not take place, as confirmed in both the height and phase images (Figure 4h). This observation clearly indicates that inked molecules need to possess C−X multiple bonds (X = C or O) to undergo hydrosilylation with surface H−Si groups. Further support for catalytic hydrosilylation-mediated pattern formation was gathered based upon the following observations: (1) When a SiO_x/Si surface was used in place of a H-terminated Si surface, no pattern was observed. Because of the lack of surface H−Si groups, alkene/alkyne/aldehyde molecules cannot link to the surface through hydrosilylation. (2) The Pt catalytic stamp could be reused multiple times without significant loss of the stamping quality (14 times; Supporting Information, Figure S5). (3) The catalytic nature of Pt nanostructures could be chemically deactivated. When a Pt catalytic stamp was immersed in a 1 mM ethanolic solution of 1-octadecanethiol for 24 h, followed by thorough rinsing with EtOH, no pattern was observed on the stamped surface because of the formation of a self-assembled monolayer on Pt (44), which blocks contact between the Pt catalyst, the ink molecules, and the surface H−Si groups.

XPS analysis also agreed with the incorporation of molecules on the H-terminated Si surface via catalytic hydrosilylation. We used 1*H*,1*H*,2*H*-perfluoro-1-decene as a demonstrative molecule because of the high loading of F atoms that are distinguishable from adventitious C 1s and O 1s. In addition, F atoms have a greater sensitivity factor (1) than that of other heteroatoms (0.42 for N atoms, for example) (45), which makes detection easier even with the low coverage of the stamped molecules relative to the entire area of a surface. After 1*H*,1*H*,2*H*-perfluoro-1-decene was stamped on an Si(111)-H surface, the sample was rinsed with CH_2Cl_2 to eliminate any physisorbed molecules on the surface and immediately loaded on a sample holder, and then the XPS spectra were recorded (Figure 5). As shown in Figure 5a, an expected single peak appeared at 688 eV, a typical value for F 1s (46). This peak was not observed with a control sample, where 1*H*,1*H*,2*H*-perfluoro-1-dodecene was stamped with a flat PDMS stamp having no imbedded Pt catalysts, indicating that the simple physisorp-

Scheme 2. Outline for Catalytic Stamp Lithography[a]

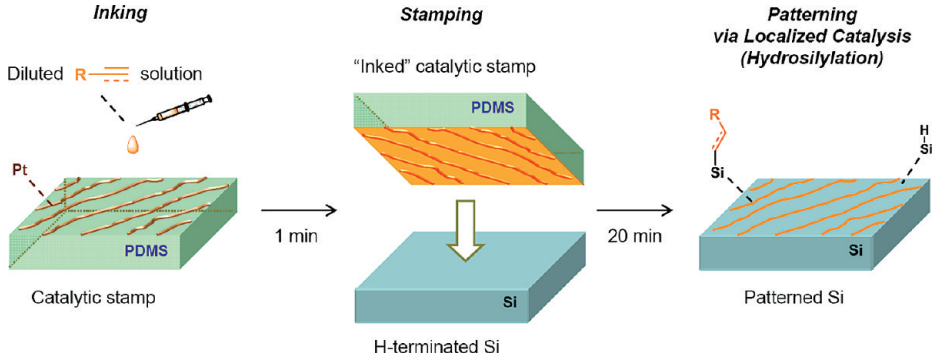

[a] In the typical procedure, a molecular ink diluted in 1,4-dioxane was first applied on a Pt catalytic stamp for 1 min. After the remaining ink was gently blown off by a nitrogen stream, the inked stamp was brought into contact with a freshly prepared H-terminated Si(111) or (100) surface for 20 min. During this stamping, molecular patterns were formed by catalytic hydrosilylation, which took place only underneath patterned Pt (localized catalysis).

tion is not sufficient to produce this level of peak intensity. In Figure 5b, the Si 2p peak found at 99.3 eV was attributed to bulk Si (40), and no significant peaks from silicon oxide (~103 eV) (40) and PDMS (~102 eV) (39) were detected. Furthermore, significant Pt leaching was not observed in the Pt 4f spectrum (Figure 5c). Together with these findings, the reusability of stamps (vide supra) led us to use the word "catalytic hydrosilylation" as an origin of pattern formation events here. A detailed study is, however, ongoing in our group to clarify whether the surface chemistry outlined here is Pt-mediated, or indeed Pt-catalyzed.

It should be noted that successful stamping is dependent upon a number of specific conditions. First, 1,4-dioxane was used as a diluent of ink molecules to avoid (1) PDMS swelling (significant catalytic stamp expansion was observed with hexane, toluene, or THF, for instance) (47) and (2) potentially competing reactions with hydrosilylation (such as alcoholysis of silanes when alcohols were used) (48). As for the concentration of molecular inks, 2−5 mM was found to be ideal for 1 min inking, and higher or lower than this range resulted in poor transfer of patterning. In particular, no pattern was obtained when a 15 mM solution of molecular ink was used, probably because of the excess population of inked molecules on the catalytic stamp, inhibiting sufficient contact between Pt catalysts and H−Si groups on a surface. A total of 20 min of stamping was enough to bring about catalysis regardless of the type of molecule, and longer times did not improve or affect the quality of patterning, based upon the AFM images. Shorter times, however, often resulted in poor patterning (Supporting Information, Figure S6).

The stability of the produced patterns by catalytic stamping to a variety of organic and aqueous solvents and solutions was examined by AFM to give a sense of how robust the films are. First, all of the patterns obtained with terminal alkene/alkyne/aldehyde molecules (shown in Figure 4) withstood immersion in boiling mesitylene (165 °C) for 3 h under Ar, indicating the strongly bonded covalent nature of these monolayers. Second, the treatment of patterned samples with a 1/1 mixed solution of 49% HF(aq)/EtOH (49) had differing effects, depending upon the molecular precursors: (1) Alkene/alkyne-stamped samples maintained the original patterns after immersion in the solution for 30 s because of the stability of the Si−C bond under these conditions; 2) When aldehyde-stamped samples were tested under the same conditions, however, the original patterns vanished because of the lability of the Si−O bonds in the presence of HF (43b). Similar trends were observed with the treatment of a Si etching solution. Figure 6 shows typical AFM height images of stamped Si(100)-H_x surfaces followed by etching treatment for 30 s with 4 M KOH(aq) containing 15% 2-propanol (50). In Figure 6a, lines produced through hydrosilylation of phenylacetylene were observed to act as a crude etch stop, with the AFM line profiles showing trench formation between the organic monolayer lines (27). No residual features were visible with a benzaldehyde-stamped sample, as shown in Figure 6b.

Finally, "inverted" catalytic stamp lithography was attempted on alkene-terminated sufaces using silanes as molecular inks. This inverted system, in principle, should also produce patterned surfaces via hydrosilylation mediated by a Pt catalytic stamp. An alkene-terminated surface was prepared through monolayer formation of octenyltrichlorosilane on an oxide capped-Si(100) substrate in toluene. This alkene-terminated SiO_x/Si(100) was stamped for 20 min, under ambient conditions, with a Pt catalytic stamp inked for 1 min with a 5 mM solution of phenylsilane in 1,4-dioxane (Scheme 3). Interestingly, we observed no pattern formation with this system. Stamping neither for longer time (1 h) nor at elevated temperature (65 °C) resulted in pattern formation. A plausible explanation for this result might be dehydrogenative condensation of silanes in the presence of a Pt catalyst (51). What is clear is that the Pt catalytic stamp, after stamping, was covered by a significant amount of unidentified materials as observed by AFM, possibly oligomerized/polymerized phenylsilane due to dehydrogenative coupling (Supporting Information, Figure S7). A related reason could be catalyst poisoning by in situ formation of di- and trihydride silane, as described in an earlier report (42b). Replacement of phenylsilane with less reactive monosilanes, such as dimethylphenylsilane or dimethyloctadecylsilane, again did not produce patterned surfaces. As with any catalytic reaction, the potential of competing reactions and catalyst poisoning or deactivation are

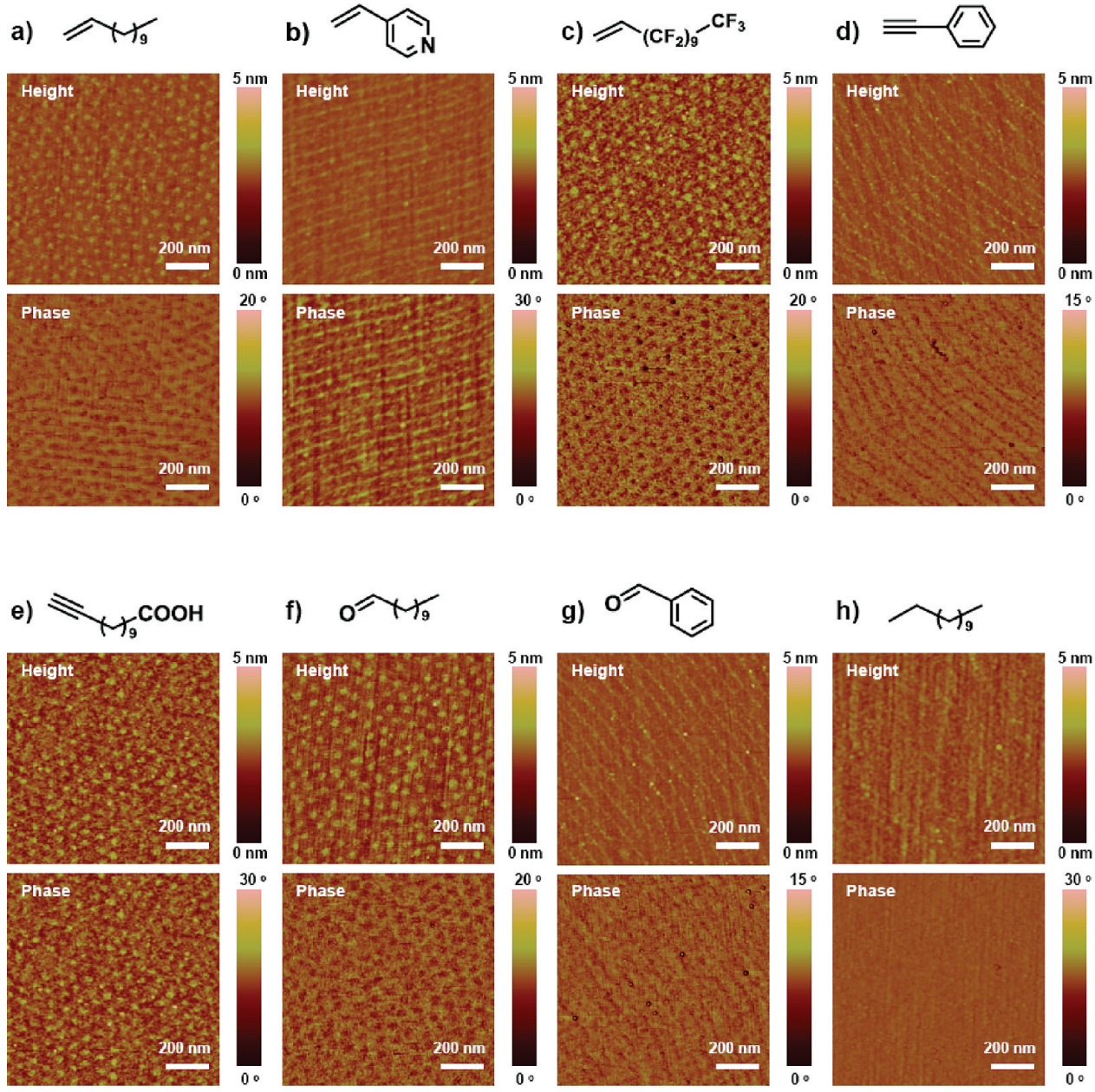

FIGURE 4. AFM height and phase images of H-terminated Si surfaces stamped with various molecular inks: (a) Si(111)-H stamped with 1-dodecene; (b) Si(111)-H stamped with 4-vinylpyridine; (c) Si(100)-H_x stamped with 1*H*,1*H*,2*H*-perfluoro-1-decene; (d) Si(111)-H stamped with phenylacetylene; (e) Si(100)-H_x stamped with 10-undecynoic acid; (f) Si(111)-H stamped with undecanal; (g) Si(111)-H stamped with benzaldehyde; (h) Si(111)-H stamped with dodecane.

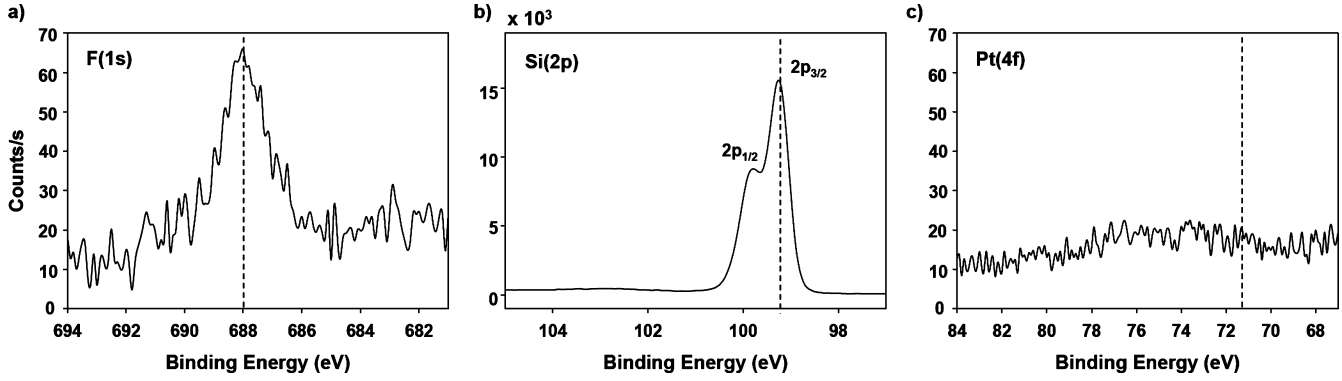

FIGURE 5. High-resolution XPS spectra of an H-terminated Si(111) surface stamped with 1*H*,1*H*,2*H*-perfluoro-1-decene: (a) F 1s region; (b) Si 2p region; (c) Pt 4f region. The dashed lines in parts a–c correspond to F (688 eV), bulk Si (99.3 eV), and metallic Pt (71.4 eV), respectively.

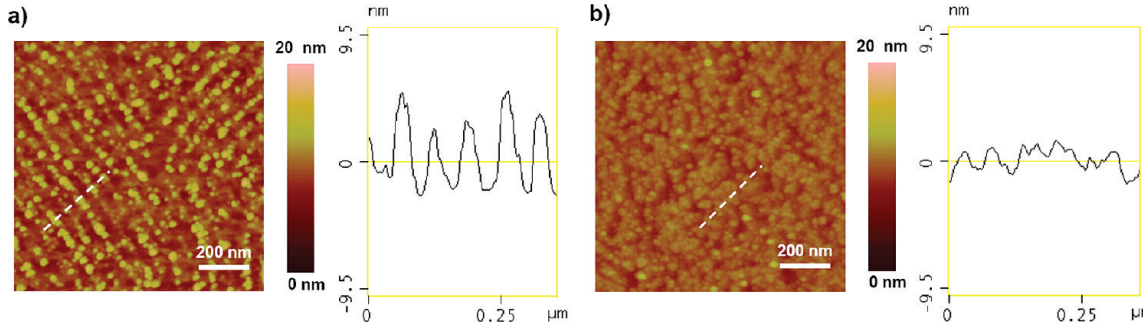

FIGURE 6. AFM height images and section analyses of H-terminated Si(100) surfaces stamped with (a) phenylacetylene and (b) benzaldehyde, followed by etching with 4 M KOH(aq) containing 15% 2-propanol for 30 s.

Scheme 3. Outline for Catalytic Stamp Lithography on an Alkene-Terminated Surface[a]

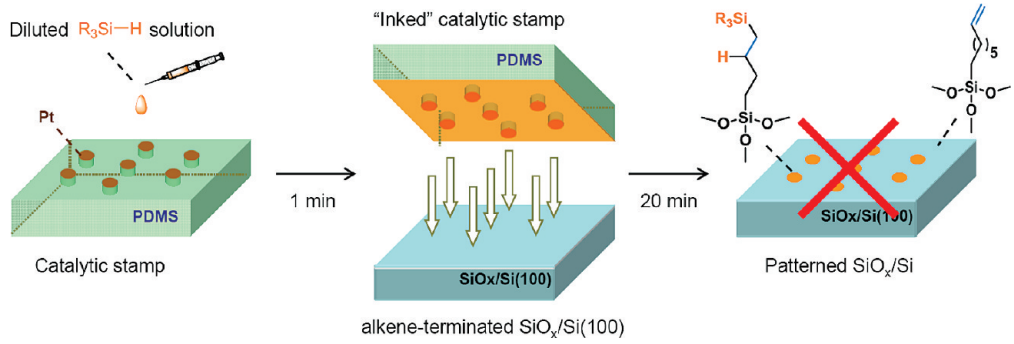

[a] A Pt catalytic stamp was inked with phenylsilane (5 mM in 1,4-dioxane) for 1 min and stamped on an alkene-terminated SiO_x/Si surface for 20 min. In this case, however, no pattern formation was observed.

always factors to consider, and thus it is necessary to carefully consider each combination of inks and surfaces to obtain successful patterning.

CONCLUSIONS

Self-assembled block copolymers were used as templates to fabricate hexagonally or linearly arranged Pt nanostructures, imbedded at the surface of PDMS. Using these hybrid materials as catalytic stamps, catalytic hydrosilylation reactions were performed on H-terminated Si surfaces and attempted on alkene-terminated oxide-capped Si surfaces. When alkene, alkyne, and aldehyde molecules were used as molecular inks, covalently attached monolayers were patterned on H-terminated Si(111) and Si(100) surfaces even at the sub-20-nm scale through highly localized catalytic hydrosilylation reactions. Because the resulting patterns maintained the same center-to-center spacing as the parent PDMS metallic stamp, stamp deformation was not a problem. All reactions were performed under ambient conditions, the resulting organic films were characterized by AFM and XPS, and a series of stability tests were designed to substantiate their identities. Catalytic stamp lithography was demonstrated to be a simple approach toward nanoscale patterning (below 100 nm), but as expected for any metal-mediated or -catalyzed reaction, competing reactions and catalyst deactivation can be a challenge.

Acknowledgment. The authors thank the NSERC, National Institute for Nanotechnology of the National Research Council (NRC-NINT), University of Alberta, and CFI for financial support. The authors are also thankful for technical support from NINT (for SEM) and the Alberta Center for Surface Engineering and Science (for XPS).

Supporting Information Available: Additional discussion on the morphological control of the polymer template (Figure S1), AFM images/data (Figures S2—S7), and XPS data (Figure S8). This material is available free of charge via the Internet at http://pubs.acs.org.

REFERENCES AND NOTES

(1) (a) Menard, E.; Meitl, M. A.; Sun, Y.; Park, J. U.; Shir, D. J. L.; Nam, Y. S.; Jeon, S.; Rogers, J. A. *Chem. Rev.* **2007**, *107*, 1117–1160. (b) Natan, A.; Kronik, L.; Haick, H.; Tung, R. T. *Adv. Mater.* **2007**, *19*, 4103–4117. (c) Aswal, D. K.; Lenfant, S.; Guerin, D.; Yakhmi, J. V.; Vuillaume, D. *Anal. Chim. Acta* **2006**, *568*, 84–108.

(2) (a) Koos, C.; Vorreau, P.; Vallaitis, T.; Dumon, P.; Bogaerts, W.; Baets, R.; Esembeson, B.; Biaggio, I.; Michinobu, T.; Diederich, F.; Freude, W.; Leuthold, J. *Nat. Photon.* **2009**, *3*, 216–219. (b) Hecht, J. *Laser Focus World* **2008**, *44*, 123–126.

(3) (a) Mela, P.; Onclin, S.; Goedbloed, M. H.; Levi, S.; Garcia-Parajo, M. F.; van Hulst, N. F.; Ravoo, B. J.; Reinhoudt, D. N.; van den Berg, A. *Lab Chip* **2005**, *5*, 163–170. (b) Knopf, D. A.; Cosman, L. M.; Mousavi, P.; Mokamati, S.; Bertram, A. K. *J. Phys. Chem. A* **2007**, *111*, 11021–11032. (c) Kreutz, J. E.; Li, L.; Roach, L. S.; Hatakeyama, T.; Ismagilov, R. F. *J. Am. Chem. Soc.* **2009**, *131*, 6042–6043.

(4) (a) Al-Kaysi, R. O.; Muller, A. M.; Bardeen, C. J. *J. Am. Chem. Soc.* **2006**, *128*, 15938–15939. (b) Garcia-Garibay, M. A. *Angew. Chem., Int. Ed.* **2007**, *46*, 8945–8947.

(5) (a) Truskett, V. N.; Watts, M. P. C. *Trends Biotechnol.* **2006**, *24*, 312–317. (b) Weibel, D. B.; DiLuzio, W. R.; Whitesides, G. M. *Nat. Rev. Microbiol.* **2007**, *5*, 209–218. (c) Lee, S. W.; Oh, B.-K.; Sanedrin, R. G.; Salaita, K.; Fujigaya, T.; Mirkin, C. A. *Adv. Mater.* **2006**, *18*, 1133–1136.

(6) (a) Geissler, M.; Xia, Y. *Adv. Mater.* **2004**, *16*, 1249–1269. (b) Pease, R. F.; Chou, S. Y. *Proc. IEEE* **2008**, *96*, 248–270.

(7) Kapoor, R.; Adner, R. *Solid State Technol.* **2007**, *50*, 51–54.

(8) (a) Gates, B. D.; Xu, Q.; Stewart, M.; Ryan, D.; Willson, C. G.; Whitesides, G. M. *Chem. Rev.* **2005**, *105*, 1171–1196. (b) Rogers,

J. A.; Nuzzo, R. G. *Mater. Today* **2005**, *8*, 50–56. (c) Ruiz, S. A.; Chen, C. S. *Soft Matter* **2007**, *3*, 168–177.
(9) Hla, S.-W. *Jpn. J. Appl. Phys.* **2008**, *47*, 6063–6069.
(10) (a) Piner, R. D.; Zhu, J.; Xu, F.; Hong, S.; Mirkin, C. A. *Science* **1999**, *283*, 661–663. (b) Salaita, K.; Wang, Y.; Mirkin, C. A. *Nat. Nanotechnol.* **2007**, *2*, 145–155. (c) Salaita, K.; Wang, Y.; Fragala, J.; Vega, R. A.; Liu, C.; Mirkin, C. A. *Angew. Chem., Int. Ed.* **2006**, *45*, 7220–7223. (d) Mirkin, C. A. *ACS Nano* **2007**, *1*, 79–83.
(11) International Technology Roadmap for Semiconductors, 2007; http://www.itrs.net/Links/2007ITRS/Home2007.htm.
(12) (a) Xia, Y.; Whitesides, G. M. *Annu. Rev. Mater. Sci.* **1998**, *28*, 153–184. (b) Xia, Y.; Whitesides, G. M. *Angew. Chem., Int. Ed.* **1998**, *37*, 550–575.
(13) (a) Kumar, A.; Whitesides, G. M. *Appl. Phys. Lett.* **1993**, *63*, 2002–2004. (b) Wilbur, J. L.; Kumar, A.; Kim, E.; Whitesides, G. M. *Adv. Mater.* **1994**, *6*, 600–604. (c) Quist, A. P.; Pavlovic, E.; Oscarsson, S. *Anal. Bioanal. Chem.* **2005**, *381*, 591–600. (d) Huck, W. T. S. *Angew. Chem., Int. Ed.* **2007**, *46*, 2754–2757. (e) Perl, A.; Reinhoudt, D. N.; Huskens, J. *Adv. Mater.* **2009**, *21*, 2257–2268.
(14) (a) Delamarche, E.; Schmid, H.; Bietsch, A.; Larsen, N. B.; Rothuizen, H.; Michel, B.; Biebuyck, H. *J. Phys. Chem. B* **1998**, *102*, 3324–3334. (b) Xia, Y.; Whitesides, G. M. *J. Am. Chem. Soc.* **1995**, *117*, 3274–3275. (c) Gannon, G.; Larsson, J. A.; Greer, J. C.; Thompson, D. *Langmuir* **2009**, *25*, 242–247.
(15) (a) Delamarche, E.; Schmid, H.; Michel, B.; Biebuyck, H. *Adv. Mater.* **1997**, *9*, 741–746. (b) Hui, C. Y.; Jagota, A.; Lin, Y. Y.; Kramer, E. J. *Langmuir* **2002**, *18*, 1394–1407. (c) Sharp, K. G.; Blackman, G. S.; Glassmaker, N. J.; Jagota, A.; Hui, C.-Y. *Langmuir* **2004**, *20*, 6430–6438.
(16) (a) Liebau, M.; Huskens, J.; Reinhoudt, D. N. *Adv. Funct. Mater.* **2001**, *11*, 147–150. (b) Li, H.; Kang, D.-J.; Blamire, M. G.; Huck, W. T. S. *Nano Lett.* **2002**, *2*, 347–349. (c) Liebau, M.; Janssen, H. M.; Inoue, K.; Shinkai, S.; Huskens, J.; Sijbesma, R. P.; Meijer, E. W.; Reinhoudt, D. N. *Langmuir* **2002**, *18*, 674–682. (d) Perl, A.; Peter, M.; Ravoo, B. J.; Reinhoudt, D. N.; Huskens, J. *Langmuir* **2006**, *22*, 7568–7573.
(17) (a) James, C. D.; Davis, R. C.; Kam, L.; Craighead, H. G.; Isaacson, M.; Turner, J. N.; Shain, W. *Langmuir* **1998**, *14*, 741–744. (b) Tormen, M.; Borzenko, T.; Steffen, B.; Schmidt, G.; Molenkamp, L. W. *Appl. Phys. Lett.* **2002**, *81*, 2094–2096. (c) Schmid, H.; Michel, B. *Macromolecules* **2000**, *33*, 3042. (d) Odom, T. W.; Love, J. C.; Wolfe, D. B.; Paul, K. E.; Whitesides, G. M. *Langmuir* **2002**, *18*, 5314. (e) Choi, K. M.; Rogers, J. A. *J. Am. Chem. Soc.* **2003**, *125*, 4060–4061.
(18) Li, H. W.; Muir, B. V. O.; Fichet, G.; Huck, W. T. S. *Langmuir* **2003**, *19*, 1963–1965.
(19) (a) Geissler, M.; Bernard, A.; Bietsch, A.; Schmid, H.; Michel, B.; Delamarche, E. *J. Am. Chem. Soc.* **2000**, *122*, 6303–6304. (b) Delamarche, E.; Donzel, C.; Kamounah, F. S.; Wolf, H.; Geissler, M.; Stutz, R.; Schmidt-Winkel, P.; Michel, B.; Mathieu, H. J.; Schaumburg, K. *Langmuir* **2003**, *19*, 8749–8758. (c) Sharpe, R. B. A.; Burdinski, D.; Huskens, J.; Zandvliet, H. J. W.; Reinhoudt, D. N.; Poelsema, B. *J. Am. Chem. Soc.* **2005**, *127*, 10344–10349. (d) Coyer, S. R.; Garcia, A. J.; Delamarche, E. *Angew. Chem., Int. Ed.* **2007**, *46*, 6837–6840. (e) Duan, X.; Sadhu, V. B.; Perl, A.; Peter, M.; Reinhoudt, D. N.; Huskens, J. *Langmuir* **2008**, *24*, 3621–3627. (f) Zheng, Z.; Jang, J.-W.; Zheng, G.; Mirkin, C. A. *Angew. Chem., Int. Ed.* **2008**, *47*, 9951–9954.
(20) Muller, W. T.; Klein, D. L.; Lee, T.; Clarke, J.; McEuen, P. L.; Schultz, P. G. *Science* **1995**, *268*, 272–273.
(21) Blackledge, C.; Engebretson, D. A.; McDonald, J. D. *Langmuir* **2000**, *16*, 8317–8323.
(22) Peter, M.; Li, X. M.; Huskens, J.; Reinhoudt, D. N. *J. Am. Chem. Soc.* **2004**, *126*, 11684–11690.
(23) (a) Davis, J. J.; Coleman, K. S.; Busuttil, K. L.; Bagshaw, C. B. *J. Am. Chem. Soc.* **2005**, *127*, 13082–13083. (b) Davis, J. J.; Bagshaw, C. B.; Busuttil, K. L.; Hanyu, Y.; Coleman, K. S. *J. Am. Chem. Soc.* **2006**, *128*, 14135–14141.
(24) Li, X. M.; Peter, M.; Huskens, J.; Reinhoudt, D. N. *Nano Lett.* **2003**, *3*, 1449–1453.
(25) Snyder, P. W.; Johannes, M. S.; Vogen, B. N.; Clark, R. L.; Toone, E. J. *J. Org. Chem.* **2007**, *72*, 7459–7461.
(26) Spruell, J. M.; Sheriff, B. A.; Rozkiewicz, D. I.; Dichtel, W. R.; Rohde, R. D.; Reinhoudt, D. N.; Stoddart, J. F.; Heath, J. R. *Angew. Chem., Int. Ed.* **2008**, *47*, 9927–9932.
(27) Mizuno, H.; Buriak, J. M. *J. Am. Chem. Soc.* **2008**, *130*, 17656–17657.
(28) (a) Glass, R.; Moeller, M.; Spatz, J. P. *Nanotechnology* **2003**, *14*, 1153–1160. (b) Albrecht, K.; Mourran, A.; Moeller, M. *Adv. Polym. Sci.* **2006**, *200*, 57–70. (c) Schulz, M. F.; Khandpur, A. K.; Bates, F. S.; Almdal, K.; Mortensen, K.; Hajduk, D. A.; Gruner, S. M. *Macromolecules* **1996**, *29*, 2857–2867.
(29) *Purification of Laboratory Chemicals*, 5th ed.; Armarego, W. L. F., Chai, C. L. L., Eds.; Elsevier: Amsterdam, The Netherlands, 2003.
(30) Kern, W. Overview and Evolution of Semiconductor Wafer Contamination and Cleaning Technology. In *Handbook of Semiconductor Wafer Cleaning Technology*; Kern, W., Ed.; Noyes Publications: Park Ridge, NJ, 1993; Vol. 3.
(31) Graham, D. J.; Price, D. D.; Ratner, B. D. *Langmuir* **2002**, *18*, 1518.
(32) (a) Higashi, G. S.; Chabal, Y. J.; Trucks, G. W.; Raghavachari, K. *Appl. Phys. Lett.* **1990**, *56*, 656. (b) Higashi, G. S.; Becker, R. S.; Chabal, Y. J.; Becker, A. J. *Appl. Phys. Lett.* **1991**, *58*, 1656.
(33) (a) Yang, W.; Yang, C.; Sun, M.; Yang, F.; Ma, Y.; Zhang, Z.; Yang, X. *Talanta* **2009**, *78*, 557–564. (b) Shiju, N. R.; Guliants, V. V. *Appl. Catal., A* **2009**, *356*, 1–17. (c) Rostovshchikova, T. N.; Smirnov, V. V.; Gurevich, S. A.; Kozhevin, V. M.; Yavsin, D. A.; Nevskaya, S. M.; Nikolaev, S. A.; Lokteva, E. S. *Catal. Today* **2005**, *105*, 344–349.
(34) (a) Aizawa, M.; Buriak, J. M. *Chem. Mater.* **2007**, *19*, 5090–5101. (b) Chai, J.; Wang, D.; Fan, X.; Buriak, J. M. *Nat. Nanotechnol.* **2007**, *2*, 500–506. (c) Chai, J.; Buriak, J. M. *ACS Nano* **2008**, *2*, 489–501. (d) Chai, J.; Taschuk, M. T.; Brett, M. J.; Buriak, J. M. *Proc. SPIE* **2008**, *7041*, 704111.
(35) (a) Spatz, J. P.; Mossmer, S.; Hartmann, C.; Moller, M.; Herzog, T.; Krieger, M.; Boyen, H.-G.; Ziemann, P.; Kabius, B. *Langmuir* **2000**, *16*, 407–415. (b) Kaestle, G.; Boyen, H.-g.; Weigl, F.; Lengl, G.; Herzog, T.; Ziemann, P.; Riethmueller, S.; Mayer, O.; Hartmann, C.; Spatz, J. P.; Moeller, M.; Ozawa, M.; Banhart, F.; Garnier, M. G.; Oelhafen, P. *Adv. Funct. Mater.* **2003**, *13*, 853–861. (c) Glass, R.; Moeller, M.; Spatz, J. P. *Nanotechnology* **2003**, *14*, 1153–1160.
(36) Graeter, S. V.; Huang, J.; Perschmann, N.; Lopez-Garcia, M.; Kessler, H.; Ding, J.; Spatz, J. P. *Nano Lett.* **2007**, *7*, 1413–1418.
(37) (a) Ripoll, C.; Muller, G.; Selegny, E. *Eur. Polym. J.* **1971**, *7*, 1393–1409. (b) Nisit Tantavichet, M. D. P. C. M. B. *J. Appl. Polym. Sci.* **2001**, *81*, 1493–1497.
(38) Jung, G.-Y.; Li, Z.; Wu, W.; Chen, Y.; Olynick, D. L.; Wang, S.-Y.; Tong, W. M.; Williams, R. S. *Langmuir* **2005**, *21*, 1158–1161.
(39) Louette, P.; Bodino, F.; Pireaux, J.-J. *Surf. Sci. Spectrosc.* **2006**, *12*, 38–43.
(40) Wagner, C. D.; Naumkin, A. V.; Kraut-Vass, A.; Allison, J. W.; Powell, C. J.; Rumble, J. R. NIST X-ray Photoelectron Spectroscopy Database. *NIST Standard Reference Database 20*, version 3.5; National Institute of Standards and Technology: Gaithersburg, MD, 2007; http://srdata.nist.gov/xps/.
(41) (a) Sabourault, N.; Mignani, G.; Wagner, A.; Mioskowski, C. *Org. Lett.* **2002**, *4*, 2117–2119. (b) Hamze, A.; Provot, O.; Alami, M.; Brion, J.-D. *Org. Lett.* **2005**, *7*, 5625–5628. (c) Hamze, A.; Provot, O.; Brion, J.-D.; Alami, M. d. *Synthesis* **2007**, *2007*, 2025–2036.
(42) (a) Lewis, L. N.; Lewis, N. *J. Am. Chem. Soc.* **1986**, *108*, 7228–7231. (b) Lewis, L. N.; Uriarte, R. J. *Organometallics* **1990**, *9*, 621–625. (c) Lewis, L. N. *J. Am. Chem. Soc.* **1990**, *112*, 5998–6004. (d) Lewis, L. N.; Uriarte, R. J.; Lewis, N. *J. Catal.* **1991**, *127*, 67–74.
(43) (a) Effenberger, F.; Gotz, G.; Bidlingmaier, B.; Wezstein, M. *Angew. Chem., Int. Ed.* **1998**, *37*, 2462–2464. (b) Boukherroub, R.; Morin, S.; Sharpe, P.; Wayner, D. D. M.; Allongue, P. *Langmuir* **2000**, *16*, 7429–7434. (c) Kong, Y. K.; Kim, J.; Choi, S.; Choi, S.-B. *Tetrahedron Lett.* **2007**, *48*, 2033–2036.
(44) (a) Li, Z.; Chang, S.-C.; Williams, R. S. *Langmuir* **2003**, *19*, 6744–6749. (b) Petrovykh, D. Y.; Kimura-Suda, H.; Opdahl, A.; Richter, L. J.; Tarlov, M. J.; Whitman, L. J. *Langmuir* **2006**, *22*, 2578–2587.
(45) *Practical Surface Analysis, Volume 1, Auger and X-ray Photoelectron Spectroscopy*, 2nd ed.; Briggs, D., Seah, M. P., Eds.; John Wiley and Sons: Chichester, U.K., 1990.
(46) Cai, W.; Lin, Z.; Strother, T.; Smith, L. M.; Hamers, R. J. *J. Phys. Chem. B* **2002**, *106*, 2656–2664.
(47) Lee, J. N.; Park, C.; Whitesides, G. M. *Anal. Chem.* **2003**, *75*, 6544–6554.
(48) (a) Lukevics, E.; Dzintara, M. *J. Organomet. Chem.* **1985**, *295*, 265–315. (b) Caseri, W.; Pregosin, P. S. *Organometallics* **1988**, *7*, 1373–1380. (c) Hilal, H. S.; Rabah, A.; Khatib, I. S.; Schreiner, A. F. *J. Mol. Catal.* **1990**, *61*, 1–17.
(49) Hurley, P. T.; Ribbe, A. E.; Buriak, J. M. *J. Am. Chem. Soc.* **2003**, *125*, 11334–11339.
(50) Finnie, K. R.; Haasch, R.; Nuzzo, R. G. *Langmuir* **2000**, *16*, 6968–6976.
(51) Tanaka, M.; Kobayashi, T.; Hayashi, T.; Sakakura, T. *Appl. Organomet. Chem.* **1988**, *2*, 91–92.

AM900602M